

A Capacitance-to-Digital Converter with Sinusoidal Excitation Suitable for Series RC Sensors

Prashanth Vooka and Bobby George, *Member IEEE*

Department of Electrical Engineering, Indian Institute of Technology Madras, Chennai 600036, India.

Abstract—A new Capacitance-to-Digital Converter (CDC) applicable for series RC sensors that requires/prefers sinusoidal excitation is proposed in this paper. The CDC presented works based on a dual-slope technique and it gives a digital output as a function of unknown capacitance of a series RC sensor, i.e., a capacitive sensor with a capacitor and a resistor in series in its electrical equivalent circuit. Output of the CDC is not sensitive to the series resistor. The CDC is useful for grounded as well as floating capacitive sensors, which needs to be excited with a sine wave for best performance. Applications of such capacitive sensors include ice detection, sterility testing of packed food products, etc. A sinusoidal Howland current source can be used to excite a grounded capacitive sensor while a simple current source with a special stabilization scheme that suppresses the effect due to static errors of opamp has been developed for floating capacitive sensor and presented in this paper. A prototype of the proposed CDC for a floating capacitive sensor has been built and tested in the laboratory. Measurement results for the sensor capacitance showed a worst case error of 0.13% for a range of 100 pF, proving the efficacy of the proposed scheme.

Keywords—Capacitance-to-digital converter; capacitive sensor; floating capacitive sensor; current source for capacitive sensors.

I. INTRODUCTION

Accurate, high sensitive, reliable and less expensive sensors are required for various industrial applications such as automation, monitoring of process variables, etc. Same features hold good for requirement of sensors in consumer applications, environmental monitoring, etc. Capacitive sensors possess all these important characteristics and hence widely used in number of scientific and industrial applications. Depending upon the dielectric used, or characteristic of the material under test, the capacitive sensor can be modeled using equivalent circuits in two distinct ways. One is a series RC model shown in Fig. 1(a) which consists of sensor capacitance C_x and a series resistance R_x [1]-[3]. In this model a resistance R_p present in parallel to the sensor is neglected due to its effect being insignificant. The second model shown in Fig. 1(b) is the

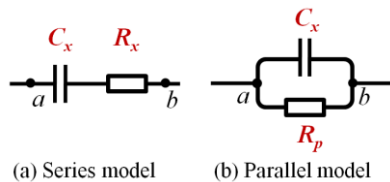


Fig. 1. Equivalent circuit of capacitive sensors. (a) RC series equivalent circuit. (b) RC parallel representation. C_x represents the sensor capacitance while R_x and R_p indicate the resistor in the series and parallel model, respectively.

parallel RC model consisting of the sensor capacitance C_x with a parallel resistance R_p . In this case the effect of the series resistance is neglected. This model is a representation for capacitive sensors used in applications such as humidity sensing [4], flow measurement, etc. Most of the available measurement schemes provide capacitance value of the sensor in a parallel model [5]. A CDC suitable for capacitive sensors with parallel RC model is reported in [6]. There are measurement circuits [1], [7] that determine the capacitance value of the sensor in the RC series model. But these techniques do not directly give out a digital value and involve many computational steps for finding out the final value. Thus Capacitance-to-Digital Converter (CDC) that accepts a RC series sensor and provides digital value of the capacitance of the sensor will be very useful. Moreover, in many applications, a sinusoidal excitation is preferred in the measurement of capacitance of the sensors [4], [8], [9]. Thus, it will be advantageous if the CDC employs a sinusoidal excitation for the measurement. Another expected feature of such a CDC is its insensitivity to the variation in the series resistor R_x . This paper reports such a CDC that measures and provides digital value of sensor capacitance using sinusoidal excitation.

II. CAPACITANCE-TO-DIGITAL CONVERTER FOR SERIES RC SENSORS

Measurement of the parameters of a sensor represented by the RC series model usually involves passing a known current through the sensor and recording the corresponding output voltage across the sensor. With the advent of silicon technology current sources can be easily realized using opamp circuits. In this paper two types of current sources are considered, based on the type of the sensor employed. The first

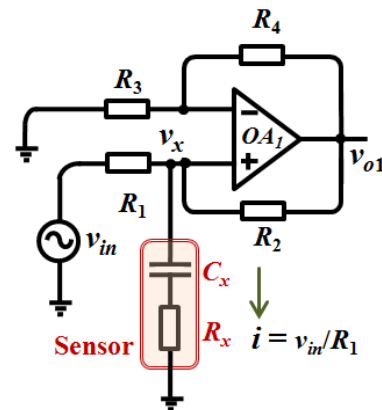


Fig. 2. Howland current source [10] injecting current v_{in}/R_1 into the capacitive sensor, represented by series RC model.

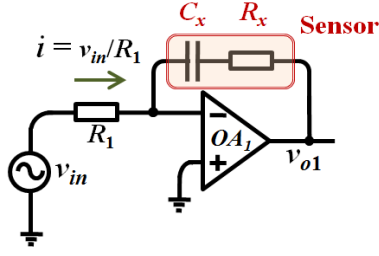


Fig. 3. A simple circuit that can inject a current of v_{in}/R_1 to a capacitive sensor (C_x and resistance R_x in series) and provides a voltage v_{o1} , which is a function of C_x . Output of this circuit, will go to saturation due to the static errors such as bias current and offset voltage of practical opamps.

is a Howland current source [10] (vide Fig. 2) which is used for grounded capacitive loads. A current i given by v_{in}/R_1 (when $R_1R_4 = R_2R_3$) flows through the sensor causing a voltage drop v_x across it. The output $v_{o1} (= 2v_x)$ can be given to the proposed converter that will return a digital count corresponding to the value of the sensor capacitance. Measurement circuits based on Howland current source are presented in [11], [12]. Precise matching of resistors is essential for the Howland current source to work efficiently. In case of any mismatch, the current drawn would be influenced by the (load) capacitive sensor [12]. Also the input bias current of the opamp needs to be as low as possible as they tend to saturate the opamp when used for capacitive loads. This is due to the fact that the output impedance offered by the Howland current source is very high in case of dc input [12].

The second current source is for a floating capacitive sensor. A simple circuit that can inject a current v_{in}/R_1 to the sensor and cause a voltage drop (in voltage v_{o1}) across it, which vary as a function of change in the capacitance C_x is shown in Fig. 3. The voltage v_{o1} for a $v_{in} = V_m \sin \omega t$ is given by

$$v_{o1} = -(R_x / R_1) V_m \sin \omega t + (1 / \omega C_x R_1) V_m \cos \omega t. \quad (1)$$

In (1), $\omega = 2\pi f_{in}$, where f_{in} is the frequency of input excitation. This circuit suffers from static errors of practical opamp. Its output will go to saturation due to bias current of opamp OA_1 , which passes through the sensor. In order to solve this problem, a modified topology, discussed below is developed.

A. Modified Current Source for Floating Capacitive Sensors

This scheme uses a simple feedback circuit to avoid the effect of static errors such as bias current and offset voltage.

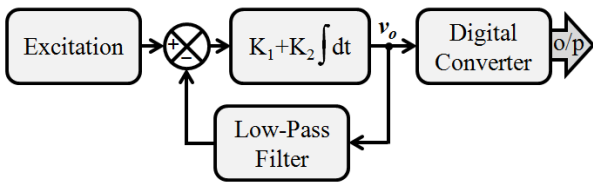


Fig. 4. Functional block diagram of the proposed capacitance-to-digital converter combined with a modified current source. It consists of an integrator with gain $K_2 = -1/R_1C_x$ and amplifier of gain $K_1 = -R_3/R_1$. The output v_o is fed as a negative feedback after passing through a low-pass filter. This eliminates the effect of static errors in the output. A digital converter is connected to output v_o which provides a digital output of unknown capacitance C_x .

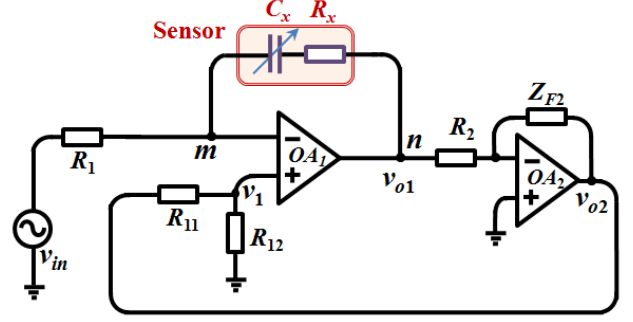


Fig. 5. Modified circuit in which output v_{o1} is filtered using an inverting low-pass filter formed by an opamp OA_2 , resistor R_2 and impedance Z_{F2} . The filtered output is fed back to the non-inverting terminal of opamp OA_1 using a resistive network. This removes the effect of bias current and offset voltage of opamp in the output voltage v_{o1} .

The block diagram of the current source followed by the converter is shown in Fig. 4. In the new scheme, the integrator output v_{o1} is passed through a low-pass filter, designed to extract the dc component present in output v_{o1} , and fed back (negative feedback) to input of opamp OA_1 . Fig. 5 shows a complete diagram of the modified circuit along with digital converter which gives the output in digital form directly proportional to sensor capacitance. A similar strategy is reported in [13] to provide bias current to an opamp. The negative feedback compensates for the effect of bias current and offset voltage of OA_1 which otherwise causes the output v_{o1} to saturate. In the modified circuit, the output v_{o1} was filtered using an inverting low-pass filter having a very low cut-off frequency and the filtered output v_{o2} is fed back to the positive terminal of opamp OA_1 using a resistive divider network as shown in Fig. 5. The voltage v_1 appearing across the non-inverting terminal will drive an opposing current due to static errors of opamp so that output v_{o1} will not go to saturation.

The inverting low-pass filter was realized using opamp OA_2 along with resistor R_2 and impedance Z_{F2} . The parameters of impedance Z_{F2} consisting of a capacitor C_{F2} with a parallel resistance R_{F2} are chosen such that the cut-off frequency of the filter, $f_{c2} (= 1/2\pi R_{F2}C_{F2})$ is set very low (close to dc). The voltage v_1 is set as $v_{o2}/2$ by choosing resistors R_{11} and R_{12} , which are equal. The dc gain of the low-pass filter is R_{F2}/R_2 .

B. Capacitance-to-Digital Converter

The complete functional diagram of the proposed capacitance-to-digital converter is shown in Fig. 6. It consists of the modified circuit (shown in Fig. 5) that passes a sinusoidal current through the sensor providing a voltage as in (1). The circuit includes the sensor having capacitance C_x and resistance R_x along with switches S_1 and S_2 and known capacitance C_S as shown in Fig. 6. An (inverting) amplifier of gain -1, SPDT switches S_3 , S_4 , opamp OA_4 , resistor R_f , capacitor C_f , comparators OC_1 , OC_2 , together with the CLU form the digital converter of the proposed CDC. Switches S_1 , S_2 , S_3 and S_4 are controlled by the CLU using control lines V_{S1} , V_{S2} , V_{S3} and V_{S4} from CLU.

The working principle of the converter is based on the popular dual-slope ADC which consists of two phases of operation, an auto-zero phase and a conversion phase. Conversion phase comprises of a preset integration period T_1

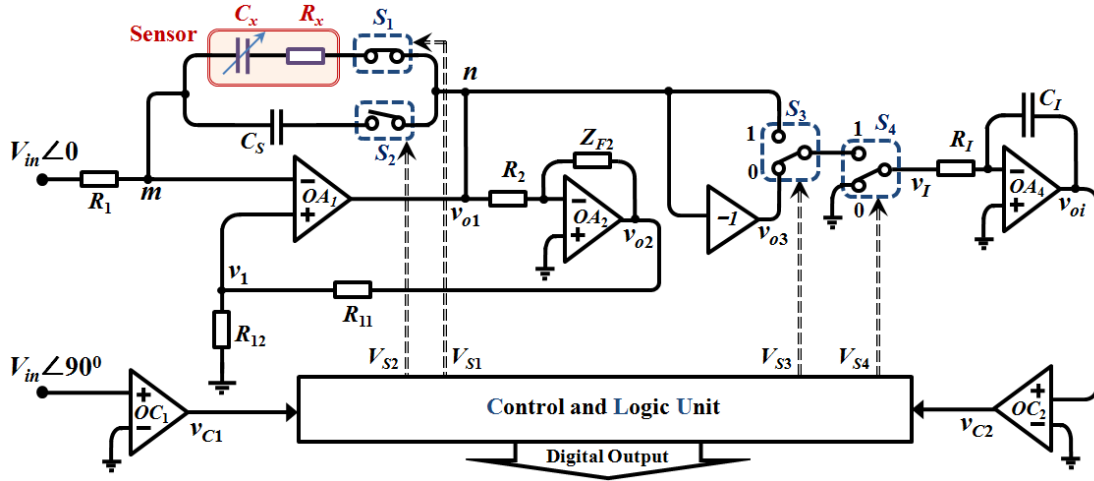


Fig. 6. Complete functional diagram of the proposed capacitance-to-digital converter consisting of the modified current source for floating capacitive loads, along with additional switches S_1 , S_2 and known capacitance C_S , integrator formed by opamp OA_4 , resistor R_l , capacitor C_l , comparators OC_1 , OC_2 and the Control and Logic Unit (CLU).

and a de-integration period of time T_2 . During the integration period T_1 , the CLU closes switch S_2 and opens switch S_1 causing a current $V_m \sin \omega t / R_1$ drawn from the excitation source $v_{in} = V_m \sin \omega t$ (where $\omega = 2\pi f_{in}$) to flow through the known capacitance C_S . The CLU also keeps switch S_4 in position-1 during T_1 .

The output v_{o1} of opamp OA_1 is given as an input to an inverting amplifier of gain -1 (formed by opamp OA_3 , two equal resistors of value R_A) and also to node-1 of switch S_3 . Further, the inverting amplifier's output v_{o3} is connected to node-0 of switch S_3 . The output voltage v_{o1} during T_1 , denoted by $v_{o1}^{T_1}$, changes due to the current flowing through C_S and is expressed in (2). The inverting amplifier's output v_{o2} ($= -v_{o1}$) during T_1 , denoted by $v_{o2}^{T_1}$, is also given in (2).

$$v_{o1}^{T_1} = (V_m / \omega C_S R_1) \cos \omega t \text{ \& } v_{o3}^{T_1} = -(V_m / \omega C_S R_1) \cos \omega t \quad (2)$$

As shown in Fig. 6, a comparator OC_1 links the CLU to the v_{in} with a phase shift of 90° . The CLU looks at the output of comparator OC_1 and whenever it is high, sets switch S_3 in position-1, otherwise holds it at position-0.

Thus, for the first positive half cycle of input excitation, i.e., from time $t = 0$ to $T_C/2$ (where $T_C = 1/f_{in}$), output v_{C1} is high only during $t = 0$ to $T_C/4$, so switch S_3 is kept in position-1 for this time connecting output $v_{o1}^{T_1}$ to the integrator (formed by opamp OA_4 , resistor R_l and capacitor C_l). A current $I_{T1} = (V_m / \omega C_S R_1 R_l) \cos \omega t$ flows through resistor R_l and also charges the capacitor C_l . At $t = T_C/4$, output v_{C1} becomes low, so CLU changes switch S_3 to position-0 causing a current $-I_{T1}$ to charge C_l in the same direction but from signal $v_{o3}^{T_1}$. The integrator output v_{oi} changes by V_{K1} (vide Fig. 7) during the first positive half cycle of v_{in} which can be derived by substituting $v_{o1}^{T_1}$ and $v_{o3}^{T_1}$ in (3).

$$V_{K1} = \Delta v_{oi} \Big|_{t=0}^{t=T_C/2} = \frac{-1}{R_l C_l} \left[\int_0^{T_C/4} v_{o1}^{T_1} dt + \int_{T_C/4}^{T_C/2} v_{o3}^{T_1} dt \right] \quad (3)$$

$$V_{K1} = -(2V_m / \omega^2 R_1 R_l C_l C_S) \quad (4)$$

Signal v_{C1} continues to be low till time $t = 3T_C/4$ and the capacitor C_l continues to charge from output $v_{o3}^{T_1}$ as the switch S_3 is still in position-0. From $t = 3T_C/4$ to T_C , v_{C1} is high, which causes the CLU to move switch S_3 to position-1. Now current I_{T1} charges the capacitor C_l from signal $v_{o1}^{T_1}$.

During the negative half cycle of v_{in} , i. e., from $t = T_C/2$ to T_C , output v_{oi} changes by the same amount V_{K1} . So, after the completion of one input excitation cycle, the charge accumulated in the capacitor C_l is $2V_{K1}C_l$. This process continues for several excitation cycles till CLU counts time $t = T_1$ ($= N_1 T_C$, where count N_1 represents the number of excitation cycles of v_{in} during T_1). At the end of the integration period the total charge stored in C_l will be

$$Q_{T_1} = 2N_1 V_{K1} C_l. \quad (5)$$

As soon as integration period ends, the CLU puts switch S_4 in position-0 connecting the input of integrator to ground and then closes switch S_1 and opens switch S_2 (make before break arrangement is provided to avoid amplifier OA_1 to operate in open loop mode). The switch S_4 is connected to position-0 for a short time T_o so that any switching transients that occur will not be reflected in the integrator output v_{oi} . The time T_o is given by $N_o T_C$ where N_o represents number of excitation cycles during which switch S_4 is in position-0. After CLU counts time T_o , switch S_4 is brought back to position-1. Now, current $V_m \sin \omega t / R_1$ flows through the sensor (capacitance C_x with a series resistance R_x) causing output voltage of OA_1 to change by $v_{o1}^{T_2}$, i. e. v_{o1} during T_2 . This voltage can be represented as in (6), which is also same as (1).

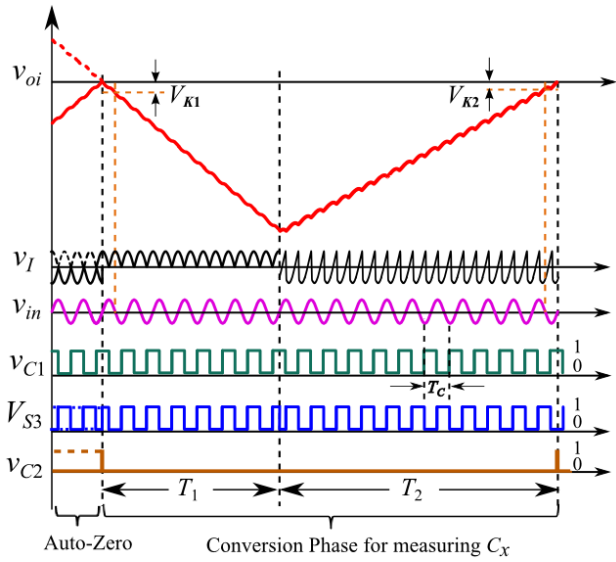


Fig. 7. Waveforms at cardinal points in the CDC, when the value of resistance R_x is equal to $1/\omega C_x$ (this condition is arbitrarily chosen and the proposed method is independent of this condition). Auto zero phase and the conversion phase for the measurement of sensor capacitance C_x are also shown. As the signal v_I is a unidirectional sine wave, the integrator voltage changes in a non-linear fashion during a half cycle of an input excitation. This is visible in v_{oi} waveform. In the derivations, charge transferred per half cycle of excitation is used, hence this non-linearity within the cycles introduce no error when T_1 and T_2 has no partial cycles. Associated error in case of a partial cycle in T_2 will be negligible when a large number of input excitation cycles are used within a conversion phase.

$$v_{oi}^{T_2} = -\frac{R_x}{R_1} V_m \sin \omega t + \frac{1}{\omega C_x R_1} V_m \cos \omega t \quad (6)$$

In the de-integration period, the CLU puts switch S_3 in position-0 whenever v_{C1} is high and in position-1 otherwise. For $v_{in} > 0$, the output v_{C1} is high from time $t = T_1$ to $T_1 + T_C/4$, so CLU sets S_3 in position-0 giving signal $v_{o3}^{T_2}$ ($= -v_{oi}^{T_2}$) to integrator formed by opamp OA_4 . This causes a current $I_{T2} = -(R_x/R_1 R_I) V_m \sin \omega t + (1/\omega C_x R_1 R_I) V_m \cos \omega t$ to flow through resistor R_I and charge the capacitor C_I . As output v_{C1} becomes low from $t = T_1 + T_C/4$ to $T_1 + T_C/2$, S_3 is moved to position-1. A current $-I_{T2}$ flows through R_I from $v_{oi}^{T_2}$ and charges capacitor C_I . The change V_{K2} in output v_{oi} during the positive half cycle of input excitation is given by

$$V_{K2} = \Delta v_{oi} \Big|_{t=T_1}^{t=T_1+T_C/2} = \frac{-1}{R_I C_I} \left[\int_{T_1}^{T_1+T_C/4} v_{o3}^{T_2} dt + \int_{T_1+T_C/4}^{T_1+T_C/2} v_{oi}^{T_2} dt \right] \quad (7)$$

By substituting $v_{oi}^{T_2}$ and $v_{o3}^{T_2}$ in (7), we get V_{K2} as

$$V_{K2} = (2V_m / \omega^2 R_1 R_I C_I C_x). \quad (8)$$

The switch S_3 continues to be in position-1 as v_{C1} is still low. The same current $-I_{T2}$ charges C_I till time $t = T_1 + 3T_C/4$ when v_{C1} becomes high and CLU changes switch S_3 to position-0. Now a current I_{T2} from $v_{o3}^{T_2}$ charges C_I till the end of the excitation cycle. During the negative half cycle the

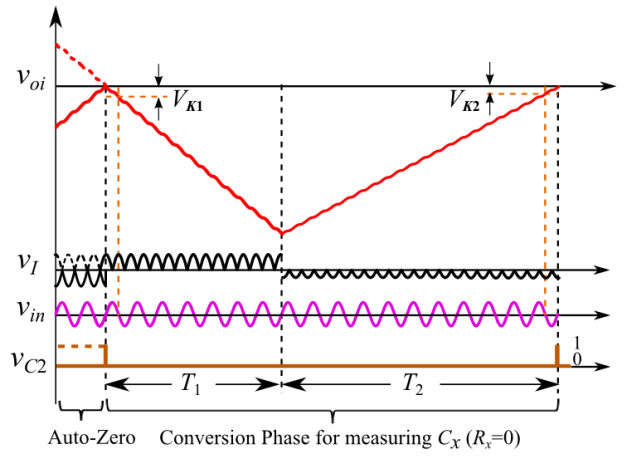


Fig. 8. Waveforms at cardinal points in the CDC, when the value of series resistance R_x is equal to zero (C_x alone is present).

output v_{oi} changes by V_{K2} . The charge acquired by capacitor C_I for one excitation cycle of v_{in} during T_2 is $2V_{K2}C_I$. The CLU continues to change (as described above) the position of switch S_3 till output v_{oi} reaches zero. The CLU notes the time T_2 ($=N_2 T_C$, where N_2 is number of excitation cycles present in T_2) when v_{oi} becomes zero. The CLU recognizes the end of de-integration period from a low to high transition at the output v_{C2} of comparator OC_2 . The total charge Q_{T_2} (refer (9)) deposited on the capacitor C_I during T_2 is equal to the charge Q_{T_1} acquired during T_1 giving the relation $|Q_{T_1}| = |Q_{T_2}|$. By substituting the values of V_{K1} and V_{K2} in the charge balance equation, we get (10).

$$Q_{T_2} = 2N_2 V_{K2} C_I \quad (9)$$

$$\frac{N_1}{C_S} = \frac{N_2}{C_x} \quad (10)$$

$$C_x = \frac{N_2}{N_1} C_S \quad (11)$$

Thus the unknown sensor capacitance C_x can be obtained in digital domain directly, by reading the de-integration count N_2 and multiplying it with a factor C_S/N_1 which is a constant as both C_S and N_1 are known fixed values. It can also be observed that (11) is not sensitive to change in the series resistance R_x . Fig. 8 shows waveforms at the important points in the CDC when the sensor resistance is set as zero. By comparing Fig. 8 and Fig. 7, we can see that the time taken for de-integration T_2 is same with and without the sensor resistance R_x .

Prior to conversion phase an auto-zero operation is performed so as to ensure that output v_{oi} is zero before the start of the conversion cycle. In auto-zero phase, CLU switches S_1 OFF and S_2 ON. It then looks at output v_{C2} , if v_{oi} is greater than 0, then $v_{C2} = 1$, and CLU sets S_3 in position-1 for v_{C1} high and in position-0 otherwise. For $v_{oi} < 0$, $v_{C2} = 0$, now the CLU sets S_3 in position-0 for v_{C1} high and in position-1 otherwise. This operation of the CLU causes output v_{oi} to bring to zero. The end of the auto-zero phase is detected by the CLU from a high to low transition if $v_{oi} > 0$ and a low to high transition if $v_{oi} < 0$.

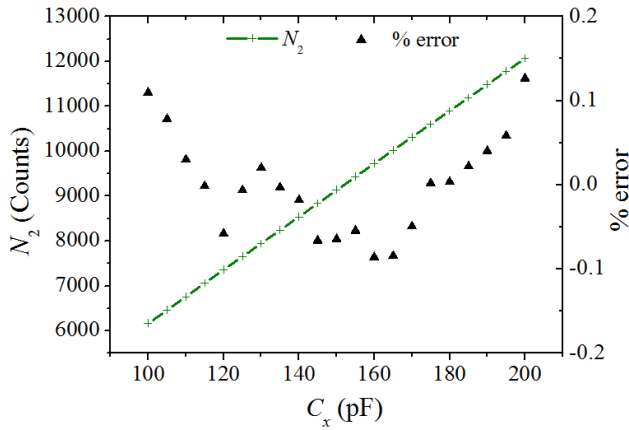


Fig. 9. Digital output N_2 obtained from the counter of CLU when sensor capacitance C_x was varied. Error for each reading is also shown.

III. EXPERIMENTAL SETUP AND RESULTS

A prototype of the proposed CDC has been built and tested in the laboratory. Values of the components used in the prototype were $R_f = 220 \text{ k}\Omega$, $C_f = 1 \text{ }\mu\text{F}$, $R_A = 27 \text{ k}\Omega$ and known capacitance $C_S = 100 \text{ pF}$. Opamps were realized using the low offset IC OPA227. Switches S_1 and S_2 were implemented using low ON resistance SPST IC MAX4601. Switches S_3 and S_4 were realized using SPDT switch IC CD4053. The task of the comparator was accomplished using high speed comparator IC LM311. The 90° phase shift was obtained using an all-pass filter. The function of the CLU was realized using a microcontroller IC MSP430G2553. A frequency 8.192 kHz (derived from a crystal clock of $32,768 \text{ kHz}$) was utilized as the clock to the counter in the CLU. The integration preset count N_1 was set at 6144 so that there are integer number of excitation cycles present during integration. The excitation frequency employed was 1 kHz . The low-pass filter for the modified current source was designed with a cut-off frequency of about 0.5 Hz . A dc gain of 15.6 was set using the resistor R_2 and fed back to the non-inverting terminal of opamp OA_1 ($R_{11} = R_{12} = 330 \text{ k}\Omega$). In order to emulate the sensor, a standard capacitance box having an accuracy of $\pm 0.01\%$ manufactured by Neptun, Geretsried, Germany was selected and connected in series to a fixed resistance $R_x = 56.250 \text{ }\Omega$. The value of the resistance was measured using a 6-1/2 digit multimeter manufactured by Agilent Technologies. A snapshot of the output v_{oi} along with the output of comparator OC_2 , for one conversion cycle is shown in Fig. 10. After completion of the integration and the

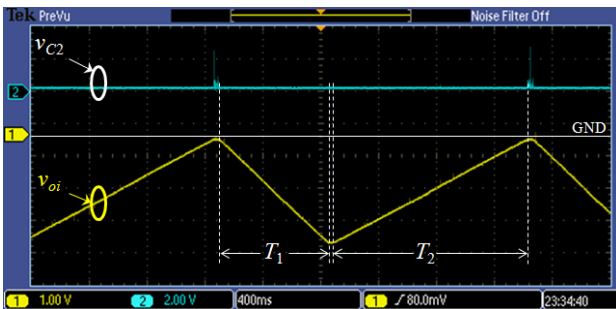


Fig. 10. Snapshot of output voltage v_{oi} along with comparator output v_{C2} of the CDC. T_1 and T_2 represent integration and de-integration periods of a conversion phase.

de-integration periods the CLU sets switch S_4 in position-0 (connecting input of integrator OA_4 to ground) for a predefined time T_o so that any switching transients that occur during T_o in the outputs of v_{o1} and v_{o3} will not affect integrator voltage v_{oi} . This short duration between T_1 and T_2 is visible in Fig. 10. The capacitance C_x was varied from 100 pF to 200 pF in steps of 5 pF and its corresponding digital output count N_2 was recorded. Percentage error with respect to the full-scale count was calculated for each change in the sensor capacitance C_x and plotted along with acquired digital output N_2 in Fig. 9. Worst case error noted for the measurement of capacitance was found to be 0.13% showing the efficacy of the proposed CDC.

IV. CONCLUSION

A new capacitance-to-digital converter that directly reads the digital value of capacitance of a series RC sensor is demonstrated. This CDC is well suited for all types of capacitive sensors and especially for sensors that prefer a sinusoidal excitation for improved performance. A prototype of the CDC has been developed and interfaced with a standard variable capacitor, along with a series resistor and tested in the laboratory. The CDC measured the capacitance accurately and its practicality has been established.

V. REFERENCES

- [1] S. N. Nihtianov, G. P. Shterev, B. Iliev and G. C. M. Meijer, "An interface circuit for R-C impedance sensors with a relaxation oscillator," *IEEE Trans. Instrum. Meas.*, vol. 50, no. 6, pp. 1563-1567, Dec. 2001.
- [2] S. N. Nihtianov and G. C. M. Meijer, "Nondestructive on-line sterility testing of long shelf-life aseptically packed food products by impedance measurements," *Proc. IEEE Autotestcon*, San Antonio, Tx, Aug. 30-Sept. 2, 1999, pp. 243-249.
- [3] S. N. Nihtianov and G. C. M. Meijer, "Indirect conductivity measurement of liquids in flexible containers," in *Proc. IMTC*, vol. 2, Ottawa, ON, Canada, May 19-21, 1997, pp. 919-922.
- [4] J. Das, S. Dey, S. M. Hossain, Z. M. C. Rittersma, and H. Saha, "A hygrometer comprising a porous silicon humidity sensor with phasedetection electronics," *IEEE Sensors Journal*, vol. 3, no. 4, pp. 414-420, Aug. 2003.
- [5] V. J. Kumar, P. Sankaran, and K. S. Rao, "Measurement of C and $\tan\delta$ of a capacitor employing PSDs and dual-slope DVMs," *IEEE Trans. Instrum. Meas.*, vol. 52, no. 5, pp. 1588-1592, Oct. 2003.
- [6] P. Vooka, A. Ranjan and B. George, "A novel capacitance-to-digital converter for capacitive sensors with AC excitation," in *Proc. 19th IMEKO TC 4 Symposium and 17th IWADC workshop*, pp. 246-249, Jul. 2013.
- [7] M. A. Atmanand, V. J. Kumar, and V. G. K. Murti, "A microcontroller based scheme for measurement of L and C," *Meas. Sci. Technol.*, vol. 6, pp. 576-581, 1995.
- [8] B. George, H. Zangl, T. Bretterkieber and G. Brasseur, "A combined inductive-capacitive proximity sensor for seat occupancy detection," *IEEE Trans. Instrum. Meas.*, vol. 59, no. 5, pp. 1463-1470, May 2010.
- [9] D. Goeger, M. Blankertz and H. Woern, "A tactile proximity sensor", *proc. of IEEE Sensors 2010*, pp. 589-594, 1-4 Nov. 2010.
- [10] Application note, 2013, AN-1515, "A comprehensive study of the Howland current pump". [Online]. Available: www.ti.com/lit/an/snoa474a/snoa474a.pdf
- [11] R. Nerino, A. Sosso, and G. B. Picotto, "A Novel AC Current Source for Capacitance-Based Displacement Measurements," *IEEE Trans. Instrum. Meas.*, vol. 46, no. 2, pp. 640-643, Apr. 1997.
- [12] D. X. Chen, X. Deng and W. Q. Yang, "Comparison of three current sources for single-electrode capacitance measurement," *Rev. Sci. Instrum.* 81, 034704 (2010).
- [13] M. A. Krupka, "Low noise, electric field sensor," U.S. Patent 7 088 175, Aug. 08, 2006.